

# MULTI-OBJECTIVE MODELING AND OPTIMIZATION OF THE THERMAL BEHAVIOR OF AN AT10-TYPE BELT TRANSMISSION USING ANOVA, RMS AND DF METHODS

Original scientific paper

UDC:621.85.052.44:66-965.11

<https://doi.org/10.46793/aeletters.2024.9.3.1>

Abdelhak Haroun<sup>\*1</sup>, Sidi Mohammed Merghache<sup>1</sup>

<sup>1</sup>Laboratory of Mechanical Engineering, Materials and Structures, Tissemsilt University, Algeria

## Abstract:

This research work focuses on the analysis of the impact of different parameters, such as the angular speed  $N_1$ , the resistant torque  $M_2$  and the setting tension  $T$  of the timing belt on its operation. The main objective is to optimize the performance of the belt by understanding how these parameters influence its thermal behaviour. By carefully examining these factors, it becomes possible to identify the adjustments needed to improve the overall efficiency of the belt. An in-depth statistical analysis was conducted using three different approaches: analysis of variance (ANOVA), response surface method (RSM) and desirability function (DF) method, in order to examine the temperature of the heating of the belt  $T_1$  and its efficiency  $\eta$ . Data from the experiment are examined and manipulated to develop mathematical models that demonstrate the correlation between various parameters and growth rates. The results clearly demonstrate that the resistant couple  $M_2$  plays a preponderant role, with contributions of 55.25% and 69.82%, respectively. In addition, the  $N_1$  angular speed also has a significant influence, contributing 7.58% and 17.84%, respectively. On the other hand, setting tension  $T$  makes a small contribution to the temperature of belt  $T_1$ . And a strong influence of 21.91% on their performance. These results clearly indicate that better efficiency can be obtained by reducing the angular speed  $N_1$  and increasing the resistive torque  $M_2$ . These results show that the developed models have been well established and that there is a good correlation between the experimental and predicted data.

## ARTICLE HISTORY

Received: 26 April 2024

Revised: 11 June 2024

Accepted: 22 July 2024

Published: 30 September 2024

## KEYWORDS

Toothed belt, Efficiency, Optimization, Measure, Temperature, Angular speed, Resistant torque

## 1. INTRODUCTION

Belt manufacturers are well aware of the importance and valuable advantages of this transmission element. They make every effort to develop and improve its geometric and mechanical properties in order to guarantee optimal long-term use [1-4]. Binder Magnetic type synchronous belts are specially designed to meet the needs of machine manufacturers operating in various fields such as textiles, machine tools, automobiles, office automation, medical, agriculture, food, transport or packaging.

The belts offer the same advantages as a single belt (flat, trapezoidal or toothed) [5,6] due to their lightweight and minimal maintenance. Its wide linear speed range and high gear ratio benefit from the advantages of a chain: absence of slip, synchronous speed transmission and low installation voltage, among others. Eighty years ago, numerous studies were carried out both theoretically and experimentally in order to better understand the behaviour of synchronous belts, with the aim of optimizing their lifespan and improving their

\*CONTACT: Abdelhak Haroun, e-mail: [abdelhak.haroune@univ-tissemsilt.dz](mailto:abdelhak.haroune@univ-tissemsilt.dz)

efficiency [7]. Scientifically, this research has played a crucial role in solving problems related to synchronous belts by shedding light on different aspects of their behaviour. The analysis of the work carried out on the belt transmission made it possible to obtain data on the static, dynamic and thermal aspects observed. It is important to note that the conditions of use have a significant impact on the behaviour of synchronous belts. Belt-driven machines are inevitably subject to wear, temperature variations and friction [8,9]. Thus, maintaining an adequate level of friction is essential to ensure efficient, slip-free power transmission. However, excess friction can lead to overheating, causing premature belt wear.

A relatively large number of articles present multidisciplinary research studies on both static and dynamic domains. Kubas presented two studies; the first [10] presents a research device for measuring static and dynamic friction parameters between the belt and pulley in a belt transmission. This device can be rebuilt in three custom configurations: static friction, kinetic and dynamic friction characteristics, and complete belt transmission. The results obtained from these bench tests will allow the development of simplified empirical models of friction between the belt and pulley in the transmission, which should improve the efficiency of calculations during dynamic analyses. In the second study [11], the author presented the results of experimental measurements of static friction forces between a 5pk poly-V belt and a pulley at a specialized research stand. It assumed an average effective static coefficient as a function of wrap angle and preload force. Kubas used the Nelder-Mead optimization method to approximate the measured results using a nonlinear function and obtain a good agreement. Following this, the author presented the dependence of the effective friction coefficient on the rest time. On the other hand, Wang et al. [12] developed a dynamic model of an automobile belt drive system with a non-circular gear instead of a round gear. The objective of this study was to analyze the effect of reducing the angular variation of camshafts and to numerically evaluate the dynamic performance of a belt drive system with a specific gear parameter design. The model has been divided into two distinct parts: the motor model and the belt drive model. To calculate the steady-state responses of the motor and belt drive models, the researchers used a modified incremental harmonic balance method that integrates the fast Fourier transform and Broyden's method. In 2020, Long et al. [13] developed models

for the dynamic responses of a timing belt drive system (TBDS) considering the mesh teeth model and the bilinear hysteresis model of the tensioner. They even conducted experiments to validate the developed models and study the influences of different mesh tooth models on the dynamic responses of a TBDS. A year before that, Shen et al. [14] presented a study developed a coupled FEM and DEM model to analyze the dynamic deflection of the belt. Based on the proposed strategy and procedures, the coupling was implemented with a focus on the challenges associated with data exchange and continued analysis. The coupling of the FEM and DEM model was used to study the dynamic deflection of two varieties of belts with distinct properties and transporting coal and iron ore. The simulation results demonstrated satisfactory agreement with the experimental data.

Research into the thermal behaviour of belts is still limited in terms of the amount of work carried out. A study by Li et al. [15] experimentally and numerically examined the heat generation and transfer phenomena in nonlinear 8M synchronous belt transmission in depth using the FEA method. The researchers developed two models using commercial ABAQUS software: the first model is a sequential thermo-mechanical coupling model for the steady-state belt. In contrast, the second model is used for thermal analysis, simulating the production and transfer of heat from the synchronous belt. A proposal was made by Zuqing et al. [16] for a coupled thermo-mechanical analysis approach of the V-belt transmission system. In this study, the V-belt geometry is described using an eight-node thermally integrated ANCF solid beam element. This approach is based on the analysis of the deformation modes of the V-belt. However, it should be noted that Merghache and Ghernaout [17] have developed a numerical model which makes it possible to estimate the heat transfer through an AT10-type pulley and belt transmission system. In 2016, research by Wurm et al. [18] focused on heat transfer analysis of continuously variable rubber belt transmissions. Using the computational fluid dynamics method, they developed a model to quantify the effects of heat transfer in a closed belt continuously variable transmission. The effect of temperature on fatigue of V-ribbed serpentine belts was studied by Sundararaman et al. [19].

These researchers developed a predictive model to evaluate the growth of cracks caused by fatigue, thus making it possible to monitor the evolution of initial defects in small ribs subjected to thermal and mechanical stress. This model is based on

computational fracture theory and fatigue tests carried out on samples subjected to different temperatures. Song et al. [20] conducted a study on the operation of a serpentine and pulley belt system equipped with ribs in a car. They developed a three-dimensional model using the dynamic finite element method, including a driving pulley, a driven pulley and a V-belt with five complete ribs. This model was integrated into the ABAQUS/EXPLICIT code to perform simulations and analyze the thermal stresses and temperature-dependent properties of rubber compounds. This approach made it possible to obtain precise and detailed results on the behaviour of the belt system under varied operating conditions. Zhang and Xia [21] developed an energy model with the aim of improving the operational efficiency of a transportation system equipped with a belt conveyor. Their approach began with the examination of existing energy models, followed by the proposal of an analytical model based on the ISO 5048 standard. This model integrates all the parameters into four coefficients which can be deduced from the design parameters or identified using a parameter identification technique.

In this article, a new method for determining the parameters that impact the thermal behaviour of an AT10-type timing belt, with a view to improving its performance is determined. Compared to previous research, a larger number of parameters, as well as their interactions, are taken into account, such as angular speed  $N_1$ , braking torque  $M_2$ , setting tension  $T$  and belt type. To achieve this, a statistical study of the results was carried out using three methods: ANOVA, RSM and DF. These analyzes made it possible to examine the heating of the belt and its performance by varying the previous operational parameters. The measurements were carried out on a test bench to evaluate the belt temperature and transmission efficiency for different configurations. The experimental results were subjected to analysis and processing to create mathematical models that help illustrate the relationship between several parameters and the rate of development. These techniques were chosen in order to determine the optimal parameters to guarantee the proper functioning of the belt.

## 2. METHODOLOGY

### 2.1 Structure and Geometry of Belts

Binder Magnetic belts are essential components in many power transmission systems, providing a low-cost, efficient means of transferring motion

between two pulleys. Made from various materials such as rubber, leather, nylon or even metal. They are designed to withstand varied operating conditions while ensuring smooth and precise transmission of motion. Whether in industrial, automatic or domestic applications, these belts play a crucial role in ensuring efficient operation of machines and equipment. These belts are made of polymers and high-strength reinforcements, which give them mechanical properties that can be adapted to all industrial applications. These transmissions are a simpler and more economical solution than a gear transmission. Furthermore, the elasticity of these elements makes it possible to absorb shocks and vibrations, which contributes to making the transmission silent and increasing its lifespan [22-24].

The dimensions and characteristics of type AT10 Fig.1-a toothed belts are described in the catalogues and various documents provided by the manufacturers. The machine designer's role is to make an informed choice based on the procedures established by the manufacturers. To succeed, it is necessary to know the operating principles and the important factors that can influence the choice of these elements [17]. These belts are armed, as standard, with zinc-plated steel cables Fig.1-b. Thanks to these cables, the belts maintain their length stability [3]. However, like any metal, steel deforms under stress following Hooke's law. This law describes the deformations under stress in the elasticity phase. The elongation of the belt will be proportional to the force in the strand [25]. These belts, obtained by linear extrusion or "endless" molding, are equipped with two types of parallel reinforcing cables.

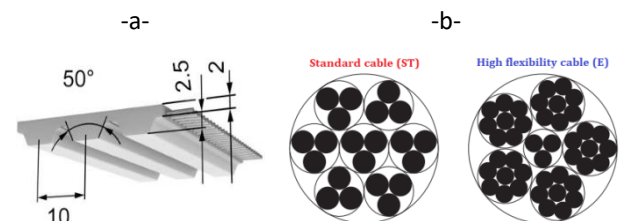


**Fig. 1.** Distribution belts Magnetic Binder: a) AT10 belt and b) the different types of belt reinforcing cables

The toothed belts, having a length of 1280 mm, a width of 32 mm, a pitch of 10 mm and a center distance of 400 mm, transmit a power  $P$ , or more precisely a torque  $M$ , through the teeth in contact  $Z_e$  on the small driving pulley of diameter  $d_{k1}$  and angular speed  $N$ . Each tooth in engagement is capable of transmitting a maximum force of  $F_{T/Z}$ . To

characterize a belt, it is therefore essential to determine the tangential force  $F_T$ , which is exerted on the teeth in contact  $Z_e$  as well as on the reinforcing cables, as illustrated in Fig. 2.

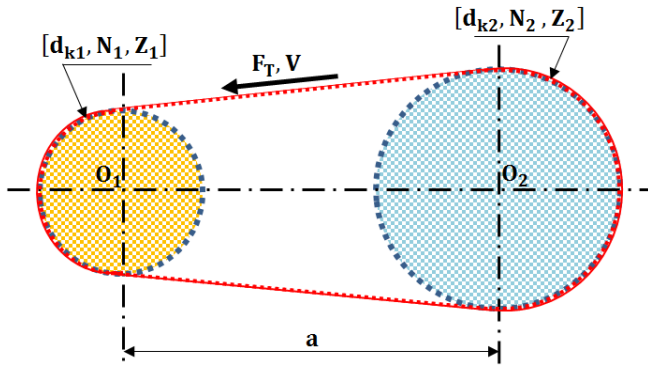


Fig. 2. Pulley-belt arrangement

The following equations Eq. (1), Eq. (2), Eq. (3), Eq. (4), Eq. (5) and Eq. (6) are used to determine the power to be transmitted  $P$  then the tangential force  $F_T$ , the linear speed  $V$ , the number of teeth engaged  $Z_e$  on the driving pulley and the resonance frequency  $f$  to adjust the setting tension  $T$  using the TSM3 device is deduced [26]:

$$M = \frac{d_{k1} \cdot F_T}{2 \cdot 10^3}, \quad (1)$$

$$P = \frac{M \cdot N}{9.55 \cdot 10^3}, \quad (2)$$

$$F_T = \frac{19.1 \cdot 10^6 \cdot P}{N \cdot d_{k1}}, \quad (3)$$

$$V = \frac{N \cdot d_{k1}}{19.1 \cdot 10^3}, \quad (4)$$

$$Z_e = \left[ \frac{Z_1}{2} - \frac{t \cdot Z_1}{2 \cdot \pi^2 \cdot a} \cdot (Z_2 - Z_1) \right], \quad (5)$$

$$f = \sqrt{\frac{1000 \cdot T}{2.5 \cdot B \cdot a^2}}. \quad (6)$$

According to the previous equations, the values of the parameters of these belts as a function of angular speed, torque and setting tension is obtained and given in Table 1.

Table 1. Calculation parameters for toothed belts

Torque (Nm)	Tangential force (N)	Angular speed (rpm)			
		1000	2000	3000	
Power (kW)	50	534	2.6	5.2	7.8
	75	1068	5.2	10.4	15.6
	100	1602	7.8	15.6	23.4
Linear speed (m/s)		2.43	4.87	7.31	
Setting tension (N)		400	500	600	
Frequency (Hz)		48.2	53.9	59	
Number of teeth		14.67 « Maximum for calculation 14 »			

## 2.2 Calculation of Efficiency and Power Losses in Toothed Belt Transmission

In order to minimise energy losses and improve the efficiency of mechanical transmissions, it is crucial to focus more on belt transmissions, as they have the capacity to generate energy savings similar to those of low-consumption motors. Over the past three decades [27,28], extensive analyzes have been conducted on power loss mechanisms, which can be divided into two main categories: torque loss and speed loss. Almeida et al. [29] also explained that torque losses mainly include hysteresis losses that occur due to bending/deflection of the belt around the pulleys. In order to minimize these losses, it is necessary to reduce the thickness of the belt or increase the diameter of the pulley to reduce stress on the belt material. An increase in drive pulley speed results in a significant increase in hysteresis power losses, which are independent of load. Then, friction losses occur between the side walls of the belt and the inner walls of the pulley each time the belt enters and exits the pulley. Finally, wind losses are associated with the kinetic energy that is transferred to the surrounding air due to belt movement. The second category of power reduction mechanism concerns speed losses, which do not manifest themselves in the timing belts and include slip and creep losses. Slippage occurs when belt tension is not sufficient to provide static friction between the belt and pulley. A study conducted by Childs and Cowburn [30] examined the effects of power loss on flat and V-belts combined with small pulleys. Their research found that belts that do not match the groove angles of their pulleys may exhibit reduced efficiency due to greater radial compliance of these belts. These results highlight the importance of precise fit between belts and pulleys to ensure optimal operation of the transmission system. Kot et al. [6] carried out a comparative analysis of the performance of three rubber V-belts for a continuously variable transmission (CVT) on a

light two-wheeled vehicle under real operating conditions.

Their measurements focused on gear ratios, overall efficiency, belt slippage and longitudinal speed. Zhu et al. [31] for their part evaluated the performance of a CVT with a rubber V-belt installed on a snowmobile. Their experimental study made it possible to measure power losses, including torque loss and speed loss and demonstrated that the efficiency of CVTs varies depending on operating conditions. Finally, Balta et al. [32] developed a V-belt drive test setup to determine the efficiency up to a torque of 200 Nm and a speed of 6000 rpm, with a fixed shaft distance. They measured braking torque as a function of slip for a single combination of belt tension, belt length, and pulley diameter.

To evaluate the efficiency of the belt drive, it is necessary to compare the output power to the input power. The low-efficiency results from large power losses, meaning that only part of the initial energy is transmitted. Adjusting the transmission parameters, such as rotational speed, torque, installation tension, and friction coefficient, makes it possible to improve the overall efficiency of the system. This approach saves energy and ensures more efficient power transmission. In this context, power losses can be classified into two categories: torque losses and speed losses. The transmitted power  $P$  can be calculated as follows:

$$P = \frac{\pi \cdot N \cdot M}{30}. \quad (7)$$

Consequently, the transmission efficiency  $\eta$  is represented by:

$$\eta = \frac{N_2 \cdot M_2}{N_1 \cdot M_1}. \quad (8)$$

The variables  $N_1$  and  $N_2$  refer to the rotational speeds of the drive pulley and the driven pulley, while  $M_1$  and  $M_2$  refer to the motor torque and the resistive braking torque, respectively. The fact that  $M$  and  $N$  are variable over time, the differentiation of the equation above leads to the relation:

$$dP = M \cdot dN + N \cdot dM. \quad (9)$$

The results of Eq.(7) and Eq.(9) show that the power losses are the sum of the torque losses and the speed losses:

$$\frac{dP}{P} = \frac{dM}{M} + \frac{dN}{N}. \quad (10)$$

### 3. EXPERIMENTAL STUDY

The study focuses on the analysis of the impacts of various parameters on the thermal behaviour of a toothed belt transmission, with the configuration presented in Fig.3. An AT10 type belt (5), with a trapezoidal profile (20° angle, 10 mm pitch), is used to transmit power between a driving pulley (4) and a receiving pulley (6). The assembly can be moved perpendicular to the axis of the well for assembly and adjustment of the belt tension. Then, all the elements are fixed to heavy rigid support, with the two pulleys mounted on shafts (1-7) 40 mm in diameter. The belt drive is switched on by an electric motor with a maximum power of 7 kW, which is fixed on a stationary support. A frequency variation is used to control the angular speed  $N_1$  of the driving pulley (which varies between 1000 and 3000 rpm). The braking torque  $M_2$  is applied to the driven pulley using a hydraulic pump, which serves as a dynamometer. This torque varies from 50 Nm to 100 Nm. It can operate under different steady-state operating conditions by adjusting a valve; in this way, different levels of braking torque can be provided. The setting tension  $T$  of the belt is adjusted manually using a screw and nut mechanism. Its adjustment is carried out using the TSM3 device (remote sensor, measuring range: 7 to 450 Hz, precision:  $\pm 5$  Hz, and operating temperature range: 0 to 50°C) [17, 26]. The setting tension varies from 400 N to 600 N. The dynamometer is installed on a cylindrical rolling bearing (8-9). The amplitudes of the reaction forces which generate the torque are measured by the load cell mounted on this bearing.

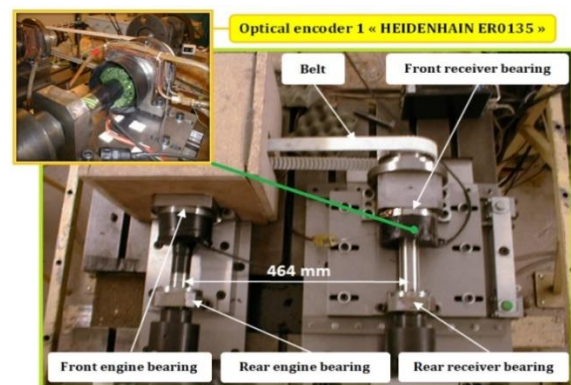


Fig. 3. The experimental setup

In this study, ignoring friction torques, the torque calculated from the force values measured on the bearing is considered equivalent to the braking torque directly applied by the dynamometer.

The rotation speeds of the driving and driven pulleys are measured using two optical encoders (10-11). It should be noted that the thermocouples

(18) are positioned at various locations on the test bench in order to monitor the thermal behaviour of the machine, particularly for the specific behaviours of our test bench. Additionally, the average belt temperature is measured using a non-contact infrared thermometer (with laser pointer, measuring range:  $-50^{\circ}\text{C}$  to  $380^{\circ}\text{C}$ , accuracy:  $\pm 1.5^{\circ}$  VS). Tests were performed for each combination of test conditions. Only one test is performed for each test condition because preliminary tests showed low dispersion of all results (less than 5%). After tension was applied, the belt ran and then resisted when the twisting moment was applied. Different values of resistance to the twisting moment were applied successively for an angular velocity. After stabilising the parameters (the 5-minute average), the measurements were carried out. Each test condition requires approximately ten minutes of testing. However, to evaluate efficiency, it is necessary to measure both the torque and speed on the motor shaft, as well as the resistive torque and speed on the slave shaft. To measure the speed of the shafts, Fig.4, optical encoders with reference HEIDENHAIN ERO1325 were used, which have a resolution of 2048 lines and a TTL output signal. These encoders are placed on the motor and receiver shaft. The data were recorded on a specific T114 digital data acquisition card, where the frequency sampling and filters were adjusted according to the signals.

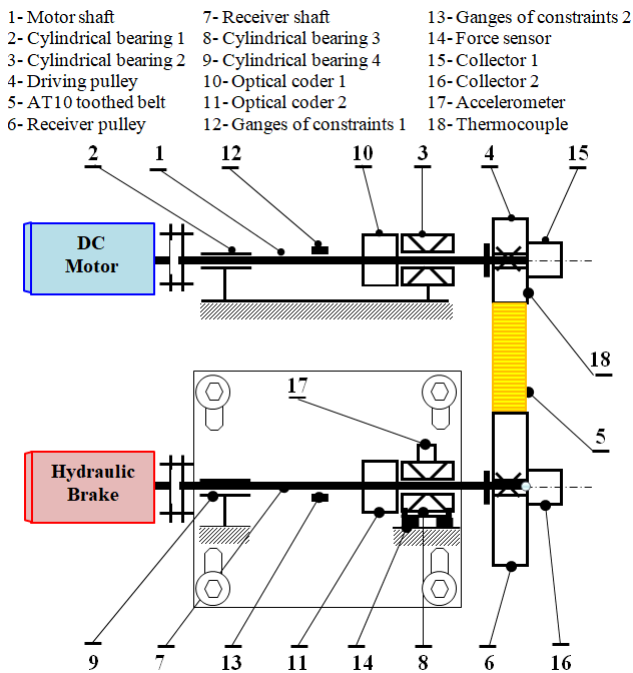


Fig. 4. Kinematic diagram of the test bench

#### 4. RESULTS AND DISCUSSION

The major objective of the tests was to determine the temperature of the belt  $T_1$  and its transmission efficiency  $\eta$  between the two pulleys (driving and receiving) for an AT10 toothed belt of the BINDER MAGNETIC type based on the Eq.(8). For this the rotational speeds of the receiver pulley  $N_2$  and the motor torques  $M_1$  from the test bench experience in the first instance was measured. These measurements are carried out under nominal conditions. Indeed, the variation of the average rotational speed of the receiving pulley  $N_2$  and the motor torque  $M_1$  as a function of time are represented by Fig.5 and Fig.6.

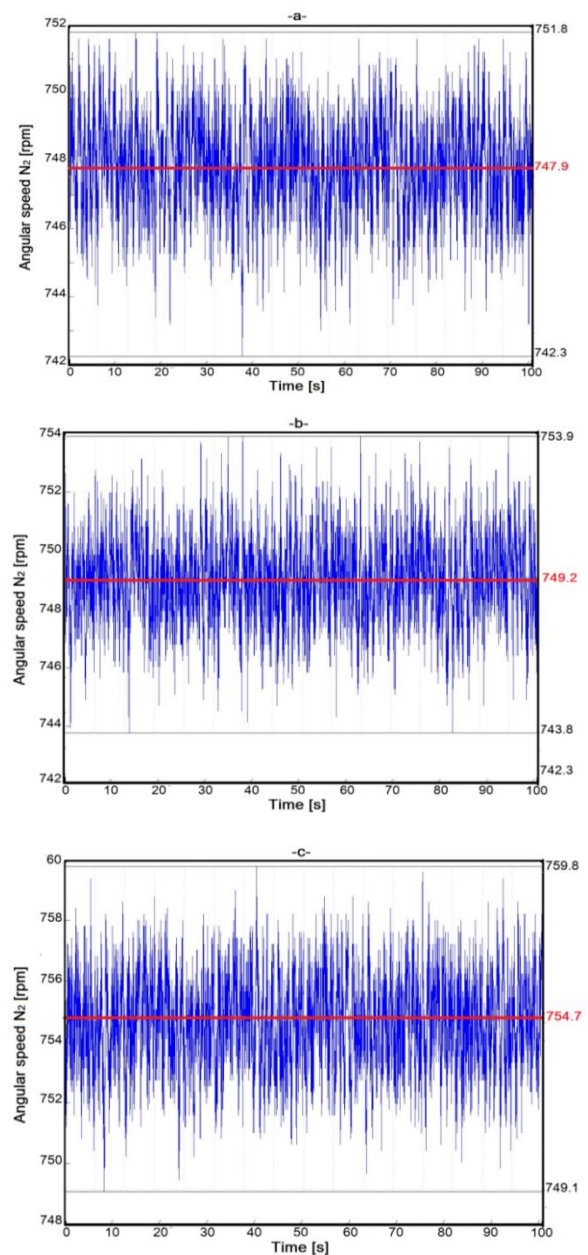
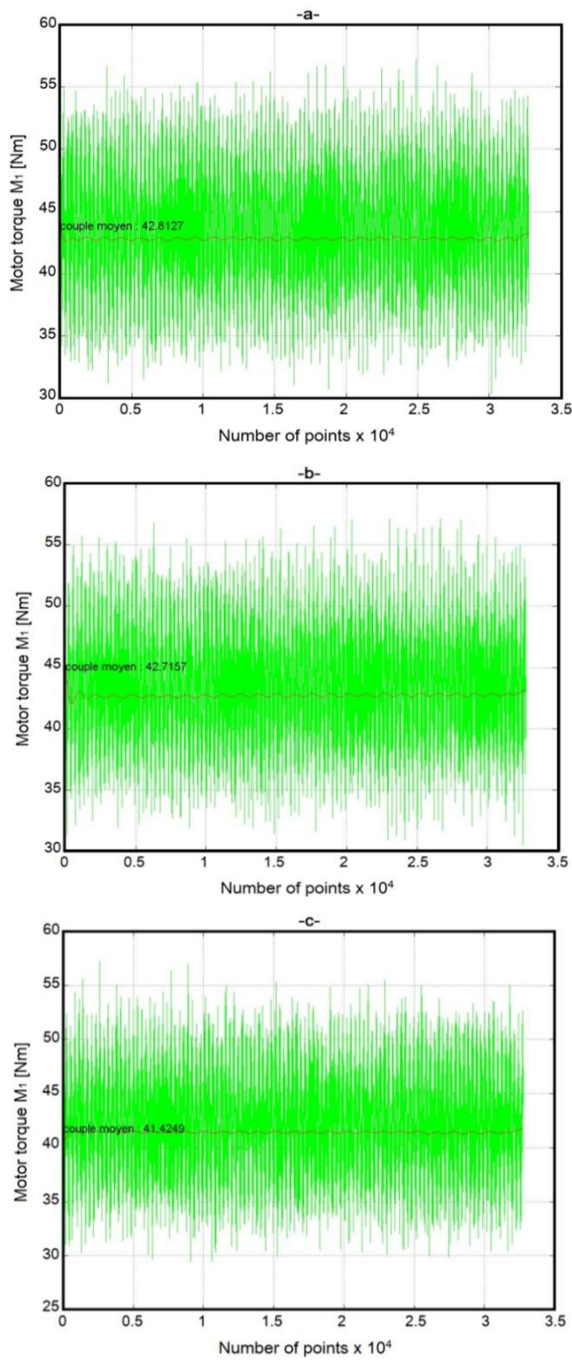


Fig. 5. The variation of the average angular speed of the receiver pulley as a function of time by AT10 belt: a)  $T = 400\text{ N}$ , b)  $T = 500\text{ N}$  and c)  $T = 600\text{ N}$



**Fig. 6.** The variation of the motor torque as a function of the number of measurement points and setting tension for an angular speed of 1000 rpm by AT10 belt: a)  $T = 400$  N, b)  $T = 500$  N and c)  $T = 600$  N

The measurement results presented in Figs. 5 and Fig.6 highlight the significant impact of the angular speed of the driving pulley  $N_1$  on the motor torque  $M_1$ . Indeed, the latter increases almost linearly with the increase in speed, going from 1000 rpm to 3000 rpm for the same resistive torque  $M_2$ . Furthermore, it is interesting to note that the differences in motor torque remain relatively constant for the three settings of tension  $T$ . The maximum values of these deviations are 5.18 Nm for  $T = 400$  N, 4.13 N for  $T =$

500 N and 6.13 N for  $T = 600$  N, which suggests a certain stability in the behaviour of the system studied. On the other hand, it is observed that the angular speed of the receiving pulley  $N_2$  only undergoes slight variations despite the increase in parameters such as the rotation speed of the driving pulley  $N_1$ , the resistant torque  $M_2$  and the setting tension  $T$ . These Speed differences are small, lying between 1.2 rpm for  $T = 400$  N, 1.5 rpm for  $T = 500$  N and 2.89 rpm for  $T = 600$  N.

The experimental results include various measurements, including belt temperature  $T_1$  and efficiency  $\eta$ . These results are based on three factors considered in this study  $N_1$ ,  $M_2$  and  $T$  in Table 2.

**Table 2.** Experimental results of  $T_1$  and  $\eta$  as a function of Operating parameters

No.	Input factors			Responses	
	$N_1$ (rpm)	$M_2$ (Nm)	$T$ (N)	Belt temperature $T_1$ (C°)	Efficiency $\eta$ (%)
1	2000	50	400	30	92.53
2	1000	75	400	33	97.48
3	2000	100	400	37	97.51
4	2000	100	600	40	97.55
5	3000	100	500	39	96.68
6	2000	50	600	36	92.65
7	3000	75	400	35	95.39
8	1000	100	500	36	98.32
9	3000	75	600	39	95.49
10	1000	75	600	37	96.90
11	1000	50	500	28	94.95
12	2000	75	500	33	96.00
13	3000	50	500	31	90.03

#### 4.1 Statistical Analysis and Modeling of Technological Parameters

Experiment planning plays a crucial role in running the experiments using the “DESIGN-EXPERT 13” software and available resources. A multiple response system is optimized, namely the belt temperature  $T_1$  and the transmission efficiency  $\eta$ , as a function of three main factors: the angular speed  $N_1$ , the resistant torque  $M_2$  and the setting tension  $T$ . The value ranges for each factor are detailed in Table 3, taking into account laboratory experience, physical resources and information published in the scientific literature for similar systems [33]. Analysis of variance (ANOVA) is a widely used statistical tool for model validation and comparison, as well as data analysis.

**Table 3.** Constraints of the optimization process

Name	Coel	Lower limit	Upper limit	Importance
$N_1$ (rpm)	in range	1000	3000	3
$M_2$ (Nm)	in range	50	100	3
$T$ (N)	in range	400	600	3
Belt temperature $T_1$ (C°)	maximize	28	40	3
Efficiency $\eta$ (%)	maximize	90.03	98.32	3

This method uses variance measures to assess the significance of the factors and the model. The interest of this analysis is to be able to absolutely test the influence of factors on the variations of a given response [33,34]. The results of the analysis are presented in Table 4 and Table 5, highlighting significant terms with a p-value less than 0.05.

**Table 4.** Analysis of variance ANOVA for belt temperature  $T_1$

Source	Sum of squares	Contribution (%)	df	Meam square	F-Value	P-Value	Noticed
Model	161.17	97.73	9	17.91	14.33	0.025	significant
$N_1$	12.50	7.580	1	12.50	10.00	0.049	significant
$M_2$	91.12	55.25	1	91.12	72.90	0.003	significant
$T$	36.13	21.91	1	36.13	28.90	0.012	significant
$N_1 \cdot M_2$	0.000	0.000	1	0.000	0.000	1.000	
$N_1 \cdot T$	0.000	0.000	1	0.000	0.000	1.000	
$M_2 \cdot T$	2.250	1.360	1	2.250	1.800	0.272	
$N_1^2$	0.321	0.190	1	0.321	0.257	0.647	
$M_2^2$	0.035	0,020	1	0.035	0.028	0.876	
$T^2$	15.75	9.550	1	15.75	12.60	0.038	significant
Residual	3.750	2.270	3	1.250			
Cor Total	164.92	100.00	12				

**Table 5.** Analysis of variance ANOVA for belt efficiency  $\eta$

Source	Sum of squares	Contribution (%)	df	Meam square	F-Value	P-Value	Noticed
Model	69.67	98.27	9	7.740	18.97	0.0177	significant
$N_1$	12.65	17.84	1	12.65	31.00	0.0114	significant
$M_2$	49.50	69.82	1	49.50	121.32	0.0016	significant
$T$	0.012	0.020	1	0.012	0.031	0.8707	
$N_1 \cdot M_2$	2.690	3.790	1	2.690	6.590	0.0827	
$N_1 \cdot T$	0.115	0.160	1	0.115	0.283	0.6314	
$M_2 \cdot T$	0.001	0.000	1	0.001	0.004	0.9540	
$N_1^2$	0.035	0,050	1	0.035	0.087	0.7866	
$M_2^2$	2.920	4.120	1	2.920	7.150	0.0754	
$T^2$	0.082	0.120	1	0.082	0.202	0.6834	
Residual	1.220	1.720	3	0.408			
Cor Total	70.90	100.00	12				

The analysis of the main factors and their interactions on  $T_1$  aims to determine their effect. From the results presented in Table 4, it is clear that the resistive torque  $M_2$  is the most determining factor for the belt temperature, with a contribution of 55.25%. Then, the setting tension  $T$  also plays an important role, with a contribution of 21.91%. On the other hand, the angular speed  $N_1$  has a weak influence, with a contribution of only 7.58%. This observation is logical because an increase in resistant torque inevitably leads to a significant

increase in belt temperature. Increasing the installation tension also leads to an increase in power and friction at the pulley bearings, which contributes to the rise in belt temperature. The contribution of the  $T^2$  interaction is estimated at 9.55%. On the other hand, the quadratic terms  $M_2 \cdot T$ ,  $M_2^2$  and  $N_1^2$  have small contributions varying from 0.02% to 1.36%. However, the terms  $N_1 \cdot M_2$  and  $N_1 \cdot T$  are not significant.

It is clear from the analysis of Table 5 that the resistant torque  $M_2$  and the angular speed  $N_1$  have

the greatest influence on the efficiency  $\eta$  of belt transmission AT10 with the respective contributions of 69.82% and 17.84%, followed by the  $M_2^2$  interaction with 4.12% contribution followed by the  $N_1 \cdot M_2$  interaction with 3.32% contribution. On the other hand, the other factors and the interactions  $T$ ,  $N_1 \cdot T$ ,  $M_2 \cdot T$ ,  $T^2$  and  $N_1^2$  do not have a significant effect since the probability value P-Value is greater than 0.05. And their contributions are low, varying from 0.01% to 0.16%. It can be noted that the increase in the resistant torque  $M_2$  leads to an increase in efficiency  $\eta$ . For its part, the increase in angular speed  $N_1$  contributes slightly to the reduction in this efficiency  $\eta$ . According to the results of the ANOVA, it is clear that the setting tension  $T$  on the efficiency is not statistically significant and that the variation in efficiency  $\eta$  with the setting tension  $T$  is a minimum of 0.02%.

The normal probability plot of the residuals of belt temperature and efficiency shown in Fig.7, and shown that the residuals (error) lie very close to the straight line of normality, proves that the limits mentioned in the first degree model are the only significant factors. Normality seems acceptable in addition to the very high correlation coefficients.

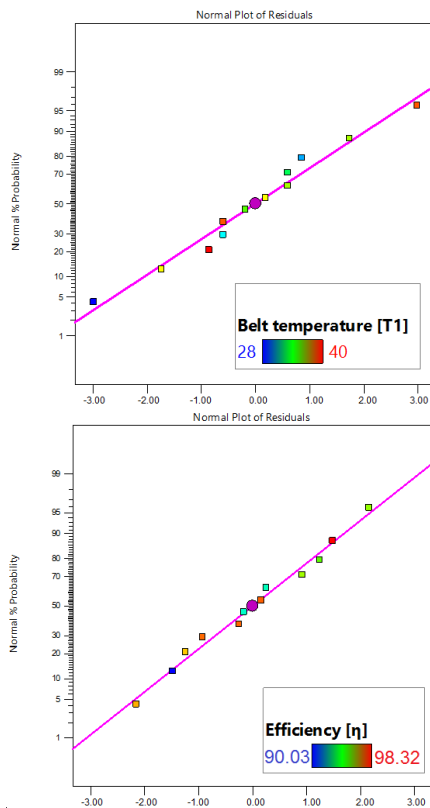


Fig. 7. Normal probabilities of the residuals of the belt temperature  $T_1$  and the efficiency  $\eta$

#### 4.2 Regression Analysis for Belt Temperature and Efficiency

Two second-order mathematical regression models were created to study the relationship between belt temperature  $T_1$  and efficiency  $\eta$ . These models were developed using Design Expert software, excluding insignificant terms and focusing only on the main effects. Thus, improved and simplified prediction models for  $T_1$  and  $\eta$  were obtained. The response variable is the belt temperature  $T_1$  and the efficiency  $\eta$ , while the predictors are the angular speed  $N_1$ , the resisting torque  $M_2$  and the setting tension  $T$ . Therefore, the equations of the fitted models in function of the real factors for the belt temperature  $T_1$  and the efficiency  $\eta$  are represented by the following two Eq.(11) and Eq.(12):

$$T_1 = 66.75 - 2.5 \cdot 10^{-4} \cdot N_1 + 0.255 \cdot M_2 - 0.218 \cdot T + 4.252 \cdot 10^{-19} \cdot N_1 \cdot M_2 + 2.177 \cdot 10^{-20} \cdot N_1 \cdot T - 3 \cdot 10^{-4} \cdot M_2 \cdot T + 3.75 \cdot 10^{-7} \cdot N_1^2 - 2 \cdot 10^{-4} \cdot M_2^2 + 2.63 \cdot 10^{-4} \cdot T^2 \tag{11}$$

Hence, its coefficient of determination  $R^2$  is 97.73%

$$\eta = 92.652 - 5.068 \cdot 10^{-3} \cdot N_1 + 0.309 \cdot M_2 - 2.22 \cdot 10^{-2} \cdot T + 3.3 \cdot 10^{-5} \cdot N_1 \cdot M_2 + 1.7 \cdot 10^{-6} \cdot N_1 \cdot T - 8 \cdot 10^{-6} \cdot M_2 \cdot T + 1.25 \cdot 10^{-7} \cdot N_1^2 - 1.808 \cdot 10^{-3} \cdot M_2^2 + 1.9 \cdot 10^{-5} \cdot T^2 \tag{12}$$

With its coefficient of determination,  $R^2$  is 98.27%.

The values of the coefficient of determination  $R^2$  for the belt temperature model  $T_1$  and the efficiency model  $\eta$  are 0.9773 and 0.9827, respectively. This means that 97.73% and 98.27% of the variations in the level of the belt temperature  $T_1$  and the efficiency  $\eta$  are explained by these two models and that 3% and 2%, therefore, remain unexplained. The adjusted coefficient of determination values of these models is  $R^2_{Adjusted} = 90.90\%$  for the belt temperature and  $R^2_{Adjusted} = 93.50\%$  for its efficiency. They represent a correction of the  $R^2$ , which allows the number of variables used in these models to be taken into consideration. They thus allow a better. Referring to two Fig.8 and Fig.9, it is possible to see that these two determination coefficients show a satisfactory correlation between the models and the simulation data. This reinforces the validity of the models established for the belt temperature  $T_1$  and the efficiency  $\eta$  by highlighting the capacity of these models to explain a large part of the variations observed.

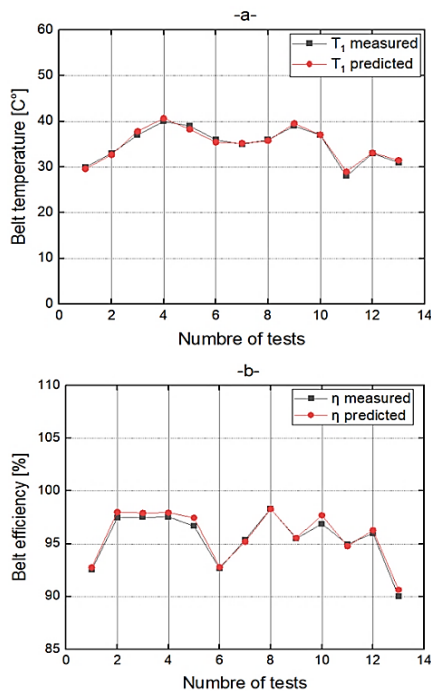


**Fig. 8.** Comparison between the measured and predicted values depending on the number of tests: a) the temperature of the belt  $T_1$  and b) the efficiency  $\eta$

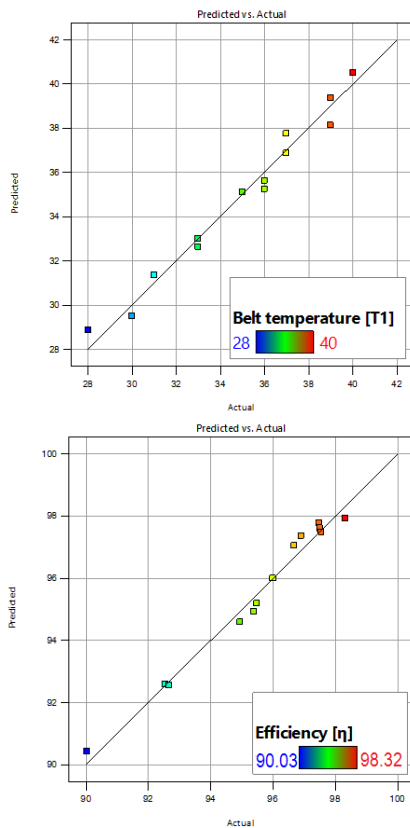


**Fig. 9.** The estimated values of the belt temperature  $T_1$  of the efficiency  $\eta$  by the equations of the models developed and the observed values

### 4.3 Analysis Using the Response Surface Method

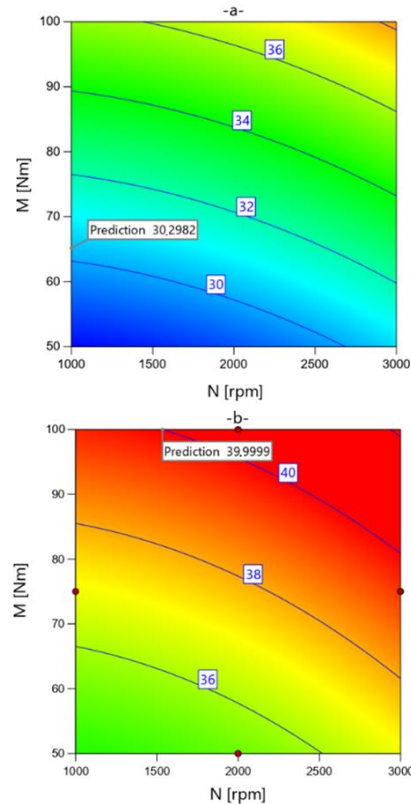
Response Surface Methodology (RSM) was used to model and analyze the operating characteristics of a belt transmission in order to minimize belt

heating and maximize its efficiency. In MSR, the quantitative form of the input ratio between the observed response and the independent variables can be represented as follows [33, 34]:

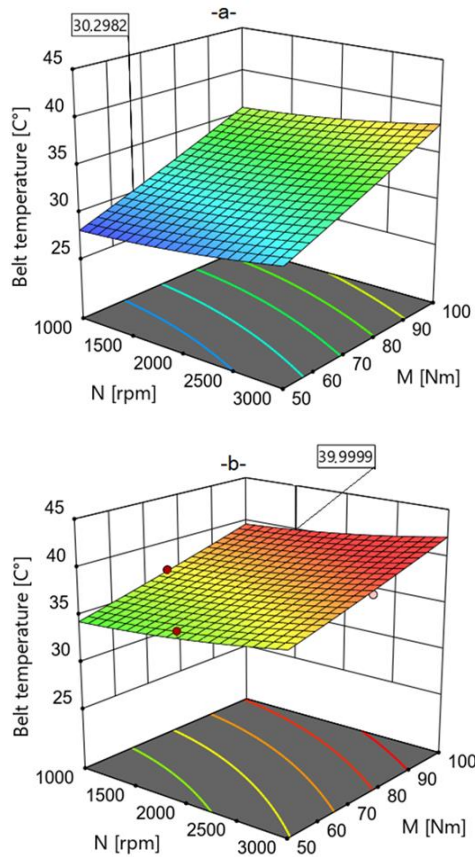
$$y = f(N_1, M_2, T), \quad (13)$$

where:  $y$  is the observed response and  $f$  is the response function (or response surface).

MSR allows the visualization of a three-dimensional (3D) plot, illustrating the response of the process as a function of two parameters but keeping the other parameters constant. In addition, Fig.10 and Fig.11 present the graphs of the 3D response surface and the 2D contours of the belt temperature  $T_1$  as a function of the parameters  $N_1$ ,  $M_2$  and  $T$ . The analysis of curves indicate that the belt temperature  $T_1$  increases significantly with the increase in the resisting torque  $M_2$  and the setting tension  $T$ . However, the angular speed  $N_1$  induces a very slight increase in the belt temperature  $T_1$ . So, it is clear that the influence of the resisting torque  $M_2$  and the installation voltage  $T$  is more important than the rotation speed  $N_1$ . Analysis of the contour graphs shows that the best (lowest) value of the belt temperature  $T_1$  is  $30.29^\circ\text{C}$ , which corresponds to the following operating speed:  $N_1 = 1000$  rpm,  $M_2 = 65.226$  Nm and  $T = 442.358$  N.



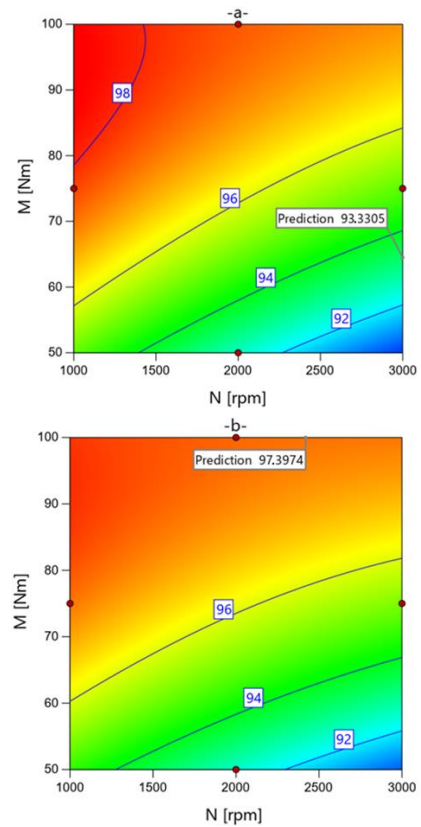
**Fig. 10.** Belt temperature contours  $T_1$  as a function of the rotation speed  $N_1$ , the resistant torque  $M_2$  and the setting tension  $T$ : a) the minimized value and b) the maximized value



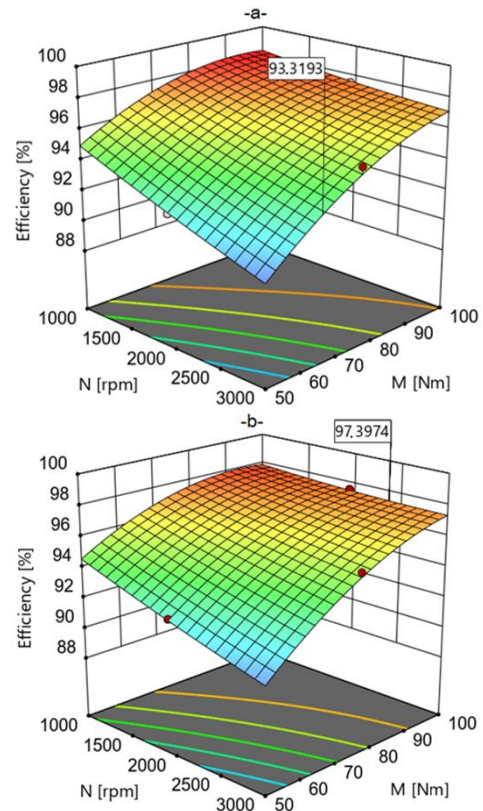
**Fig. 11.** The response surfaces of the belt temperature  $T_1$  as a function of the rotation speed  $N_1$ , the resistant torque  $M_2$  and the setting tension  $T$ : a) the minimized value and b) the maximized value

Fig.12 and Fig.13 bring together the graphs of the 3D response surface and the 2D contours of the efficiency  $\eta$  of the belt as a function of the parameters  $N_1$ ,  $M_2$  and  $T$ . It is noted that the torque resisting an impact is more significant on the efficiency  $\eta$ . This efficiency does not change much with the increase in the installation voltage but tends to almost decrease with the increase in the angular speed  $N_1$ .

This figure indicates that a better efficiency can be achieved for the smallest value of the angular speed  $N_1$  and very large values of the resistant torque  $M_2$ . So, it is clear that the influence of the resisting torque  $M_2$  is more important than the setting tension  $T$  the angular speed  $N_1$ . The analysis of the contour graphs shows that the best (highest) value of the belt efficiency  $\eta$  is 97.397%, which corresponds to the following operating speed:  $N_1=2418.724$  rpm,  $M_2=100$  Nm and  $T=599.999$  N



**Fig. 12.** Belt efficiency contours  $\eta$  as a function of the rotation speed  $N_1$ , the resistant torque  $M_2$  and the setting tension  $T$ : a) the minimized value and b) the maximized value



**Fig. 13.** The response surfaces of the belt efficiency  $\eta$  as a function of the rotation speed  $N_1$ , the resistant torque  $M_2$  and the setting tension  $T$ : a) the minimized value and b) the maximized value

To summarize, it is essential to consider the resistive torque  $M_2$  when designing and optimizing belt transmission systems, as it has a significant impact on the overall efficiency. The results obtained highlight the importance of finding an adequate balance between various parameters such as angular speed, belt tension and resistive torque in order to guarantee the correct operation and optimal performance of the system.

### 5. OPTIMIZATION OF BELT OPERATING CHARACTERISTICS

The final technique for optimizing multiple responses of a system simultaneously is the desirability function. This function allows imposing additional criteria, such as unacceptable limits and the severity with which the response must remain near the desired area. Starting from several equations expressing different responses and having common factors, it is a question of synthesizing these functions into a single one, called the composite response or desirability. Subsequently, it is sufficient to optimize it using the usual response surface techniques. Such a method becomes practically necessary when the analysis includes more than three factors. The optimal values of the characteristics  $N_1$ ,  $M_2$  and  $T$ , which produce the greatest thermal efficiency  $\eta$  with minimum belt heating  $T_1$  in order to improve the performance of belt transmissions are determined. Given the planning of the experimental design, the generated equations can be determined from prediction equations, which allow for predicting the results for a chosen set of settings. Likewise, it is possible to find the settings corresponding to the optimal responses. Simultaneous response optimization ( $T_1$  and  $\eta$ ) is performed for these purposes.

Table 3 shows the constraints used during the optimization process. Table 6 reports the optimal solutions in order of decreasing desirability. The desirability value 1 corresponds to the best value of efficiency  $\eta$  with minimum belt temperature  $T_1$  in the range of operating conditions.

The graph of the desired optimal solution is given in Fig.14. This figure shows the maximum desirability value and the values of the operating conditions  $N_1$ ,  $M_2$  and  $T$  to obtain the best performance values of a belt transmission of type AT10 (reduction in belt heating and increase in efficiency).

Table 6. Optimal solutions

Number	$N_1$ (rpm)	$M_2$ (Nm)	T (N)	Belt $T_1$ (C°)	$\eta$ (%)	Desirability
1	1000.74	91.11	410.17	34.99	98.34	1.000 Selected
2	1036.97	94.40	404.37	35.76	98.38	1.000
3	1006.17	98.09	408.42	36.24	98.32	1.000
.	.	.	.	.	.	.
95	2570.38	100.00	599.99	41.34	97.38	0.886
96	2950.02	100.00	599.99	42.03	97.35	0.883

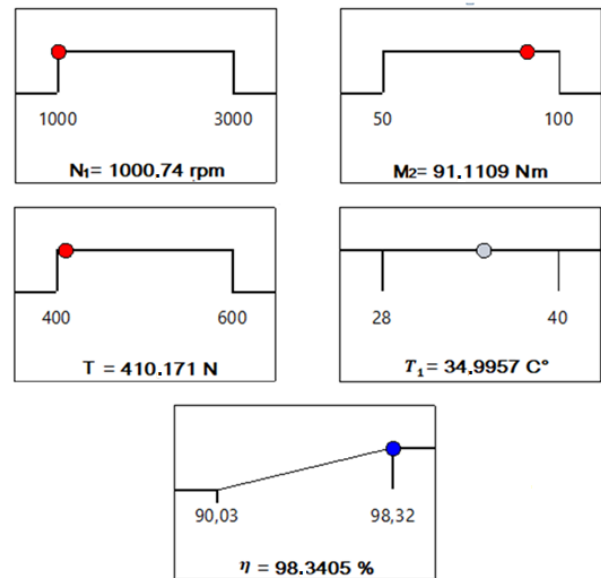


Fig. 14. Multiple response optimization diagram of belt temperature  $T_1$  and efficiency  $\eta$

### 6. CONCLUSION

This more in-depth approach allows for a better understanding of the factors influencing the thermal operation of the belt, which can lead to significant improvements in its overall performance. By considering a wider range of parameters, this study provides a more comprehensive perspective on how these variables interact and affect the thermal behaviour of the AT10-type timing belt. The main conclusions of this work are as follows:

- The ANOVA results show that the main factors influencing the belt temperature and its performance are the resisting torque  $M_2$ , with contributions of 55.25% and 69.82%, respectively. The angular speed  $N_1$  contributes 7.58% and 17.84%, respectively. However, a strong contribution of 21.91% of the setting tension  $T$  is observed on the belt temperature, while its effect on the efficiency is negligible.
- The values of the determination coefficient  $R^2$  (97% and 98%) and the adjusted determination coefficient  $R^2_{Adjusted}$  (90.90% and 93.509%) indicate

a good correlation between the belt temperature  $T_1$  and efficiency  $\eta$  models and simulation data. The correction made by the adjusted coefficient of determination allows one to take into account the complexity of the variables used in these models, which reinforces their validity and precision.

- According to the MSR method, it should be pointed out that increasing the rotational speed  $N_1$  and the resistant torque  $M_2$  have greater effects on the belt temperature  $T_1$ . On the other hand, the engine torque has a more pronounced impact on the efficiency  $\eta$ . The latter does not vary much with increasing installation voltage, but tends to decrease almost systematically with increasing angular speed  $N_1$ .
- The DF method makes it possible to obtain the optimal values of the belt operating characteristics. For example, the angular speed  $N_1$  is 1000.74 rpm, the torque  $M_2$  is 91.1109 Nm and the installation tension  $T$  is 410.171 N. Thanks to these values, it is possible to achieve an efficiency  $\eta$  of 98.3405%, while maintaining the temperature of the  $T_1$  belt at a minimum of 34.9957°C.

The results obtained thanks to our modeling made it possible to highlight a solid agreement between the values estimated by the modeling and those provided by the experiment, which underlines the advantage of the optimization technique proposed in this study.

### Conflicts of Interest

The authors declare no conflict of interest.

### REFERENCES

- [1] M. Kagotani, T. Koyama, H. Ueda, A Study on Transmission Error in Timing Belt Drives (Effect of Production Error in Polychloroprene Rubber Belt). *Journal of Mechanical Design*, 115(4), 1993:1038-1043.  
<https://doi.org/10.1115/1.2919253>
- [2] H. Tokoro, M. Nakamura, N. Sugiura, H. Tani, K. Yamamoto, T. Shuku, Analysis of Transverse Vibration in Engine Timing Belt. *JSAE Review*, 18(1), 1997: 33-38.  
[https://doi.org/10.1016/S0389-4304\(96\)00049-5](https://doi.org/10.1016/S0389-4304(96)00049-5)
- [3] M. Wilczyński, G. Domek, Influence of tension layer quality on mechanical properties of timing belts. *MATEC Web of Conference*, 254, 2019: 05010.  
<https://doi.org/10.1051/mateconf/201925405010>
- [4] N. Bojic, R. Nikolic, M. Banić, B. Hadzima, Evaluation of Mechanical Properties of the Two PVC Conveyor Belts. *Communications - Scientific Letters of the University of Zilina*, 20(4), 2018: 47-51.  
<https://doi.org/10.26552/com.C.2018.4.47-51>
- [5] P. Krawiec, Ł. Warguła, K.J. Waluś, E. Gawrońska, Z. Ságová, Z. Ságová, J. Matijošius, Efficiency and Slippage in Draw Gears with Flat Belts. *Energies*, 15(23),2022: 9184.  
<https://doi.org/10.3390/en15239184>
- [6] A. Kot, W. Grzegożek, W Szczypiński-Sala, The analysis of an influence of rubber V-belt physical properties on CVT efficiency. *IOP Conference Series: Materials Science and Engineering*, 421(2), 2018: 022017.  
<https://doi.org/10.1088/1757-899X/421/2/022017>
- [7] S. Chowdhury, R. Yedavalli, Dynamics of belt-pulley-shaft systems. *Mechanism and Machine Theory*, 98, 2016: 199-215.  
<https://doi.org/10.1016/j.mechmachtheory.2015.11.011>
- [8] Y. Huang, Y. Wu, G. Xiao, Y. Zhang, W. Wang, Analysis of abrasive belt wear effect on residual stress distribution on a grinding surface. *Wear*, 486-487, 2021: 204113.  
<https://doi.org/10.1016/j.wear.2021.204113>
- [9] B. Wang, D. Dou, N. Shen, An intelligent belt wear fault diagnosis method based on deep learning. *International Journal of Coal Preparation and Utilization*, 43(4), 2022: 708-725.  
<https://doi.org/10.1080/19392699.2022.2072306>
- [10] K. Kubas, measurement of the static friction coefficient between a poly-V belt 5pk and a pulley under dry conditions. *Tribologia*, 277(1), 2018: 57-62.  
<https://doi.org/10.5604/01.3001.0011.8290>
- [11] K. Kubas, A research stand for measuring friction parameters in a belt transmission. *The Archives of Automotive Engineering – Archiwum Motoryzacji*, 75(1), 2017: 69-83.  
<https://doi.org/10.14669/AM.VOL75.ART4>
- [12] X.F. Wang, W.D. Zhu, Dynamic Analysis of an Automotive Belt-Drive System With a Noncircular Sprocket by a Modified Incremental Harmonic Balance Method. *Journal of Vibration and Acoustics*, 139(1), 2017: 011009.  
<http://dx.doi.org/10.1115/1.4034250>

- [13] S. Long, X. Zhao, W.-B. Shangguan, W. Zhu, Modeling and validation of dynamic performances of timing belt driving systems. *Mechanical Systems and Signal Processing*, 144, 2020: 106910.  
<https://doi.org/10.1016/j.ymsp.2020.106910>
- [14] J. Shen, C. Wheeler, D. Ilic, J. Chen, Application of open source FEM and DEM simulations for dynamic belt deflection modelling. *Powder Technology*, 357, 2019: 171-185.  
<https://doi.org/10.1016/j.powtec.2019.08.068>
- [15] W. Li, X. Zhang, Y. Shang, Q. Chen, C. Chen, Z. Xin, Investigation of dynamic heat generation and transfer behavior and energy dissipation for nonlinear synchronous belt transmission. *Applied Thermal Engineering*, 144, 2018: 457-468.  
<https://doi.org/10.1016/j.applthermaleng.2018.08.080>
- [16] Y. Zuqing, C. Yaqi, Z. Qun, J. Liu, Y. Qin, Thermo-mechanical coupled analysis of V-belt drive system via absolute nodal coordinate formulation. *Mechanism and Machine Theory*, 174, 2022: 104906.  
<https://doi.org/10.1016/j.mechmachtheory.2022.104906>
- [17] S.M. Merghache, M.E.A. Ghernaout, Experimental and numerical study of heat transfer through a synchronous belt transmission type AT10. *Applied Thermal Engineering*, 127, 2017: 705-717.  
<https://doi.org/10.1016/j.applthermaleng.2017.08.079>
- [18] J. Wurm, M. Fitl, M. Gumpesberger, E. Väisänen, C. Hochenauer, Advanced heat transfer analysis of continuously variable transmissions (CVT). *Applied Thermal Engineering*, 114, 2017: 545-553.  
<https://doi.org/10.1016/j.applthermaleng.2017.12.007>
- [19] S. Sundararaman, J. Hu, J. Chen, K. Chandrashekhara, Temperature dependent fatigue failure analysis of V-ribbed serpentine belts. *International Journal of Fatigue*, 31(8-9), 2009: 1262-1270.  
<https://doi.org/10.1016/j.ijfatigue.2009.01.019>
- [20] G. Song, K. Chandrashekhara, W.F. Breig, D.L. Klein, L.R. Oliver, Analysis of cord-reinforced poly-rib serpentine belt drive with thermal effect. *Journal of Mechanical Design*, 127(6), 2005: 1198-1206.  
<https://doi.org/10.1115/1.2049088>
- [21] S. Zhang, X. Xia, Modeling and energy efficiency optimization of belt conveyors. *Applied Energy*, 88(9), 2011: 3061-3071.  
<https://doi.org/10.1016/j.apenergy.2011.03.015>
- [22] V.U. Kumaran, L. Weiss, M. Zogg, Analytical flat belt drive model considering bilinear elastic behaviour with residual strains. *Mechanism and Machine Theory*, 190, 2023: 105466.  
<https://doi.org/10.1016/j.mechmachtheory.2023.105466>
- [23] M. Batista, Elastic belt extended by two equal rigid pulleys. *Acta Mechanica*, 230, 2019: 3825-3838.  
<https://doi.org/10.1007/s00707-019-02377-z>
- [24] V. Ravindra, C. Padmanabhan, C. Sujatha, Static and free vibration studies on a pulley-belt system with ground stiffness. *Journal of the Brazilian Society of Mechanical Sciences and Engineering*, 32(1), 2010: 61-70.  
<https://doi.org/10.1590/S1678-58782010000100009>
- [25] B. Stojanović, N. Miloradović, N. Marjanović, M. Blagojević, L. Ivanović, Length Variation of Toothed Belt during Exploitation. *Journal of Mechanical Engineering*, 57(9), 2011: 648-654.  
<https://doi.org/10.5545/sv-jme.2010.062>
- [26] S.M. Merghache, A. Hamdi, M.E.A. Ghernaout, Experimental Measurement and Evaluation of the Noise Generated by Three Transmissions by Synchronous Belts of Type AT10, BAT10 and SFAT10. *International Journal of Precision Engineering and Manufacturing*, 23, 2022: 31-43.  
<https://doi.org/10.1007/s12541-021-00599-7>
- [27] S. Dereyne, E. Algoet, P. Defreyne, K. Stockman, Construction of an energy efficiency measuring test bench for belt drives. *Energy Efficiency of Motor Driven Systems, Proceedings, Rio de Janeiro, Brazil*, 2013, 1-8.
- [28] T.F. Chen, D.W. Lee, C.K. Sung, An experimental study on transmission efficiency of a rubber V-belt CVT. *Mechanism and Machine Theory*, 33(4), 1998: 351-363.  
[https://doi.org/10.1016/S0094-114X\(97\)00049-9](https://doi.org/10.1016/S0094-114X(97)00049-9)
- [29] A.D. Almeida, S. Greenberg, Technology assessment: energy-efficient belt transmissions. *Energy and Buildings*, 22(3), 1995: 245-253.  
[https://doi.org/10.1016/0378-7788\(95\)00926-0](https://doi.org/10.1016/0378-7788(95)00926-0)
- [30] T.H.C. Childs, D. Cowburn, Power transmission losses in V-belt drives Part 1: mismatched belt and pulley groove wedge angle effects.

*Proceedings of the Institution of Mechanical Engineers, Part D: Journal of Automobile Engineering*, 201(1), 1987: 33-40.

[https://doi.org/10.1243/PIME\\_PROC\\_1987\\_201\\_155\\_02](https://doi.org/10.1243/PIME_PROC_1987_201_155_02)

- [31] C. Zhu, H. Liu, J. Tian, Q. Xiao, X. Du, Experimental investigation on the efficiency of the pulley-drive CVT. *International Journal of Automotive Technology*, 11, 2010: 257-261.  
<https://doi.org/10.1007/s12239-010-0032-2>
- [32] B. Balta, F. Sonmez, A. Cengiz, Experimental identification of the torque losses in V-ribbed belt drives using the response surface method,

*Proceedings of the Institution of Mechanical Engineers, Part D: Journal of Automobile Engineering*, 229(8), 2014: 1070-1082.

<https://doi.org/10.1177/0954407014555150>

- [33] R.H. Myers, D.C. Montgomery, C.M. Anderson-Cook, *Response Surface Methodology: Process and Product Optimization Using Designed Experiments*, 2<sup>nd</sup> ed. Wiley, New Jersey, USA, 2016, p.856.
- [34] D.C. Montgomery, *Design and Analysis of Experiments*, 5<sup>th</sup> ed. Wiley, New Jersey, USA, 2000, p.724.